TIME-FREQUENCY BASED WAVEFORM AND RECEIVER DESIGN FOR SHALLOW WATER COMMUNICATIONS

Jun Zhang and Antonia Papandreou-Suppappola

Department of Electrical Engineering, Arizona State University, Tempe, AZ 85287-7206

ABSTRACT

In this paper, we propose a frequency-domain characterization of shallow water systems based on normal-mode acoustic processing that is applicable to a large class of signals. After studying the dispersive characteristics of this system, we propose a matched transmission waveform and receiver structure. The design uses a warping technique and the system characteristics to obtain time-dispersion diversity. Simulation results demonstrate that the system characterization and receiver schemes can improve processing performance.

***Index Terms*—** Time-frequency analysis, dispersive channels, underwater acoustic communication

1. INTRODUCTION

Underwater acoustic communications is challenging due to the transmitted signal's interactions with the ocean bottom and surface, dense dispersion effect in the water medium and time-varying (TV) changes of the ocean environment. Specifically, the shallow water acoustic environment is a linear TV dispersive system that shifts lower frequencies by larger amounts in time than higher frequencies [1, 2].

Recent techniques in underwater communications use space-time processing or time reversal methods to counteract distortion effects [3, 4]. On the other hand, in [2], a characterization of shallow water systems was considered that matched the dispersive signal transformation caused on the transmitted waveforms. This system was successfully used for shallow water communication to obtain time-dispersion diversity. However, this characterization was only applicable to signals with very high bandwith as it assumed that the transmitted waveform was an impulse.

In this paper, we consider a more general characterization that is applicable to a larger class of signals. Specifically, we use the normal-mode model discussed in [5] which is based on a frequency domain formulation and can be used for narrowband as well as wideband waveforms. Our objective is to design the transmitted waveform and the corresponding receiver structure for a shallow water communication system to achieve time-dispersion diversity. Specifically, both the transmitter and receiver are designed to match the dispersive characteristics of the underwater medium.

*This work was supported by the NSF CAREER Award CCR-0134002 and the Department of Defense Grant No. AFOSR FA9550-05-1-0443.

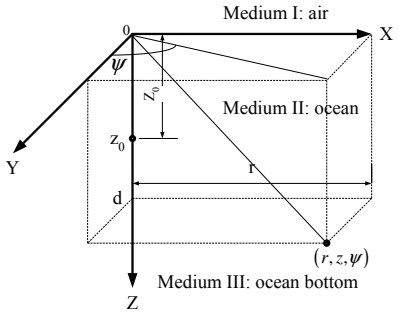

Fig. 1. Waveguide model with point source in Medium II at $r = 0$, $z = z_0$; the ocean is d m deep.

In Section 2, we discuss the normal mode-model and in Section 3, we formulate our system model in shallow water. In Section 4, we use a matched signal transform to design the transmission waveform and the corresponding receiver structure with an optimal detector. In Section 5, numerical results illustrate our improved performance.

2. UNDERWATER NORMAL-MODE MODEL

We first discuss the normal-mode model for shallow water environments following [5]. While normal modes are more commonly used as a computational tool, they are useful in the present context for their analytical properties and rich time-frequency (TF) structures. The normal-mode model treats the ocean as a waveguide with plane, parallel boundaries, representing the acoustic field in the ocean medium as a sum of normal modes. A simple waveguide model of the ocean is shown in Fig. 1 using the cylindrical coordinate system (r, z, ψ), where Medium I, II and III correspond to air, ocean water and ocean bottom, respectively. An omnidirectional point source with signal spectrum $X(f)$ is located in Medium II at $r = 0$ and $z = z_0$, and the ocean is d meters deep. We consider the sound speed in Medium II as a constant u m/s.

The ocean surface (at $z = 0$) should be realistically modeled as an ideal pressure release boundary and the ocean bot-

tom at $z = d$ as an ideal rigid boundary. However, the modeling for the ocean bottom is not realistic due to the roughness and scattering properties of the medium. The ocean waveguide problem involves the derivation of an expression for the velocity potential in Medium II (ocean water) which is a solution of the wave equation and satisfies all the boundary conditions, including the boundary condition at the source.

After a detailed derivation in [5], under the assumption of perfect waveguide, the received signal spectrum excited by $X(f)$ at location (r, ψ, z) is given by

$$Y_{ideal}(f) = X(f) \sum_{n=0}^{N_p-1} C_n \Theta_n(f). \quad (1)$$

The nth mode is characterized by

$$\Theta_n(f) = \sqrt{\frac{1}{\frac{\sqrt{f^2-f_n^2}}{u} r}}\, e^{-j2\pi \frac{r}{u}\sqrt{f^2-f_n^2}}, \quad (2)$$

where $f_n = \frac{(2n+1)u}{4d}$ is the cutoff frequency of the nth mode and N_p is the largest mode number. The parameter

$$C_n = e^{-j\frac{\pi}{4}} \frac{1}{2\pi d} \sin(\frac{(2n+1)\pi z_0}{2d}) \sin(\frac{(2n+1)\pi z}{2d}),$$

is constant for any given fixed coordinates (r, z, ψ).

From (1) and (2), the transmitted signal experiences group delay shifts given by $\frac{d}{df}\frac{r}{u}\sqrt{f^2 - f_n^2}$ within each mode, and the received signal is the summation of all the mode contributions.

3. SHALLOW WATER CHARACTERISTICS

Under the ideal waveguide assumption, the model in (1) can be seen as a perfect inherent frequency domain system model. However, in realistic shallow water environments, many factors can cause distortion in the signal propagation, e.g., the ocean surface fluctuates with the waves, and the roughness of the ocean bottom affects the signal reflections. Hence, it is reasonable to introduce randomness into the channel model. We model this distortion following the data generated by the normal-mode modeling software *KRAKEN* [6]. Specifically, we replace the constant deterministic term C_n in (2) with

$$D_n(f) = D_n A_n(f), \quad (3)$$

where $A_n(f)$ is a deterministic function that characterizes the average frequency change in the nth mode due to the mismatch between the realistic shallow water environments and the ideal model in a perfect waveguide. The random distortion D_n can be modeled with a Gaussian random magnitude with mean C_n and uniform phase. In practice, D_n and $A_n(f)$, need to be measured by conducting a system identification. Additive noise is also introduced in the channel model due to the random disturbance in the ocean environment and receiver. Hereby, the received signal spectrum is expressed as

$$R(f) = Y(f) + W(f) = X(f) \sum_{n=0}^{N_p-1} D_n(f)\Theta_n(f) + W(f), \quad (4)$$

where $W(f)$ is additive white Gaussian noise with variance σ_W^2.

The dispersive group delay nature of the nth mode can be demonstrated using simulated data from *KRAKEN*. Specifically, an example of $Y(f)$ in (4) is shown represented by its spectrogram in Fig. 2(a) for $N_p = 3$ modes. As it can be seen, lower frequencies are shifted in time by larger amounts than higher frequencies for each mode.

4. SYSTEM DESIGN FOR DIVERSITY

In order to effectively exploit the diversity offered by this dispersive system, we need to design appropriate transmission waveform and receiver schemes. Specifically, if we can separate the modes in the TF plane, we can then utilize the processing to obtain diversity from those modes.

4.1. Transmission Waveform Design

In order to separate each mode, we design the transmitted signal spectrum as $X(f) = \sqrt{f}$ for $f > f_n$. With this input, we can apply a unitary warping operation to the received signal that is specific to each mode. In particular, for the n_0th mode, we define $V_{n_0}(f) = X(f)\Theta_{n_0}(f)$, and we apply the warping operator $\mathcal{U}_{n_0}$ defined in [2] to $V_{n_0}(f)$ as

$$\begin{aligned}(\mathcal{U}_{n_0} V_{n_0})(f) &= \frac{f^{\frac{1}{2}}}{(f^2 + f_{n_0}^2)^{\frac{1}{4}}} V_{n_0}((f^2 + f_{n_0}^2)^{\frac{1}{2}}) \\ &= \sqrt{\frac{u}{r}} e^{-j2\pi f \frac{r}{u}}. \end{aligned} \quad (5)$$

This illustrates that after warping, $V_{n_0}(f)$ becomes a single impulse concentrated at $t = \frac{r}{u}$. Specifically, when the dispersive warping operation $\mathcal{U}_{n_0}$ is applied to the signal $Y(f)$, where $Y(f)$ is the noiseless received signal in (4), we have

$$\begin{aligned}\mathcal{Y}_{n_0}(f) &= (\mathcal{U}_{n_0} Y)(f) \\ &= D_{n_0} A_{n_0}((f^2 + f_{n_0}^2)^{\frac{1}{2}}) \sqrt{\frac{u}{r}} e^{-j2\pi f \frac{r}{u}} \\ &+ \sum_{n \neq n_0} D_n (\mathcal{U}_{n_0} X A_n \Theta_n)(f). \end{aligned} \quad (6)$$

Thus, this separates the n_0th mode from all other modes.

To further investigate the TF characteristics of the received signal in shallow water environments, we consider the spectrogram (squared magnitude of short-time Fourier transform) of $\mathcal{Y}_{n_0}(f)$ in Fig. 2. Specifically, the spectrograms of $\mathcal{Y}_0(f)$,

$\mathcal{Y}_1(f)$ and $\mathcal{Y}_2(f)$ are shown as Figs. 2(b), 2(c) and 2(d), respectively. Fig. 2(a) shows each mode as a dispersive (nonlinear) curve in the TF plane. The three modes in this representation are not easily separable. However, when we obtain the spectrogram of the warped signal and look at each mode separately, the corresponding mode appears as a wideband pulse. Note that the other modes (e.g., mode 1 and 2 in Fig. 2(b)) are still dispersive especially in the low frequency band. In the higher frequency section, the three modes are not separable. This is because as f increases, all three modes appear as impulses since for $f \gg f_n$, $e^{-j2\pi(\frac{\sqrt{f^2-f_n^2}}{u}r)} \approx e^{-j2\pi f\frac{r}{u}}$.

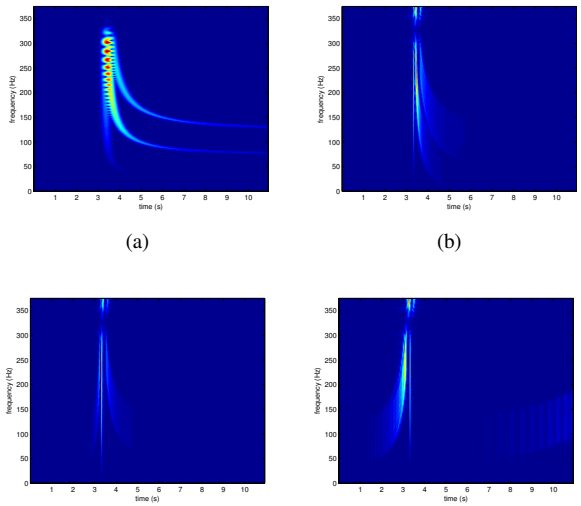

Fig. 2. Spectrogram of (a) $Y(f)$ (b)$\mathcal{Y}_0(f)$ (c) $\mathcal{Y}_1(f)$ (d) $\mathcal{Y}_2(f)$.

As we demonstrated, in the low frequency region, each mode can be discriminated by applying a corresponding warping. However, whether the modes can be separated or not also depends on the transmission band and the distance between the transmitter and receiver. Generally speaking, a longer transmission distance causes the signal to become more dispersive, so the modes are easier to discriminate. If the signal is transmitted in a high frequency band, the modes are closer to each other, and are more difficult to separate.

4.2. Receiver Design

We propose a filter bank receiver scheme which can exploit the frequency domain dispersion diversity in the normal modes. The received signal spectrum $R(f)$ in (4) is processed to separate each mode, and then the outputs are combined in the minimum-probability-of-error sense to obtain the optimal detection rule for the transmitted information symbol b. This receiver scheme is shown in Fig. 3.

As stated above, we design $X(f) = \sqrt{f}$ ($f > f_{N_p-1}$), and then we employ frequency domain matched filtering to

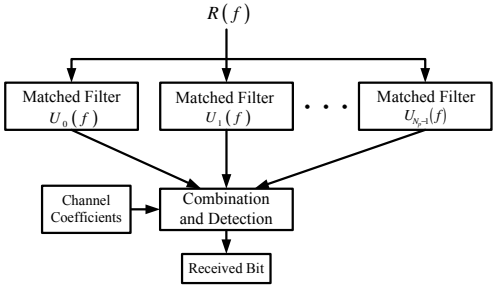

Fig. 3. A filter bank receiver scheme.

the received signal. Recalling that $D_n(f) = D_n A_n(f)$, we define $U_n(f) = \Theta_n(f)X(f)A_n(f) = V_n(f)A_n(f)$ for the nth mode. Then the noiseless output of the n_0th matched filter can be expressed as

$$Z_{n_0} = \langle Y(f), A_{n_0}(f)V_{n_0}(f)\rangle = \int_f Y(f)U^*_{n_0}(f)df. \quad (7)$$

As the warping operator $\mathcal{U}_{n_0}$ is unitary [7], we can rewrite (7) as

$$\langle Y(f), A_{n_0}(f)V_{n_0}(f)\rangle = \langle (\mathcal{U}_{n_0}Y)(f), (\mathcal{U}_{n_0}A_{n_0}V_{n_0})(f)\rangle .$$

Using (5) and (6), the output of the n_0th matched filter is

$$Z_{n_0} = \int_f (\mathcal{U}_{n_0}Y)(f)G(f)e^{j2\pi f\frac{r}{u}}df.$$

This can be seen as the short-time Fourier transform of the warped signal $(\mathcal{U}_{n_0}Y)(f)$ at epoch $\frac{r}{u}$ using an analysis window $G(f) = A^*_n(\sqrt{f^2-f_n^2})$. According to the discussion of Section 4.1, the modes can be most easily separated at this epoch in the TF plane.

This receiver processing can be described as follows. Concatenating the signals $U_n(f)$, we can express the resulting filter bank using vector $\mathbf{U}(f) = [U_0(f) \ \cdots \ U_{N_p-1}(f)]^{\mathbb{T}}$, where $\mathbb{T}$ denotes the transpose of matrices. Similarly, we rewrite b as an $N_p \times 1$ vector $\mathbf{b} = [b, \ b, \ \cdots b]^{\mathbb{T}}$. Let $\mathbf{D} = \text{diag}\,(D_0, D_1, \cdots, D_{N_p-1})$ be the $N_p \times N_p$ matrix whose diagonal elements are the random channel coefficients in (3). Using the aforementioned vector notation, the received spectrum can also be written as

$$R(f) = \mathbf{U}^{\mathbb{T}}(f)\,\mathbf{Db} + W(f). \quad (8)$$

The output of this filter bank is given by $\mathbf{Z} = \mathbf{PDb}+\mathbf{W}$, where $\mathbf{P} = \int_f \mathbf{U}^*(f)\mathbf{U}^{\mathbb{T}}(f)\,df$ is the matrix of correlations between different modes, and $\mathbf{W} = \int_f \mathbf{U}^*(f)W(f)\,df$ is the noise at the output of the matched filters with covariance $\sigma^2_W\mathbf{P}$.

If binary antipodal symbols are transmitted, i.e., $b = +1$ or -1, and we denote $\mathbf{d} = \mathbf{Db}$ using the above notation, then the communication problem stated above is converted to a classic, detection problem with hypothesis

$$\mathcal{H}_0 : \mathbf{Z} = -\mathbf{Pd} + \mathbf{W}, \quad (9)$$

$$\mathcal{H}_1 : \mathbf{Z} = \mathbf{Pd} + \mathbf{W}. \quad (10)$$

Denoting the conjugate transpose operation as $\dagger$, notice that $\mathbf{P} = \mathbf{P}^\dagger$ is a Hermitian matrix, thus it can be expressed as $\mathbf{P} = \mathbf{V}^\dagger \mathbf{\Delta} \mathbf{V}$, where $\mathbf{\Delta} = \text{diag}(\lambda_1, \lambda_2, \cdots, \lambda_{N_p})$ is the eigenvalue matrix of $\mathbf{P}$. From the properties of Hermitian matrices we also know that all the eigenvalues are greater or equal to zero. Hereby we assume $\lambda_1 \geq \lambda_2 \geq \cdots \lambda_{N_p-1} \geq \lambda_{N_p} \geq 0$, and the first N_r eigenvalues are greater than 0. We use the first N_r rows of $\mathbf{V}$ to form the new matrix $\mathbf{V}_r$ and the first N_r rows of $\mathbf{\Delta}$ to form $\mathbf{\Delta}_r$.

We can use the Bayesian approach to minimize the probability of error in the received symbols. Assuming that the probabilities of transmitting $+1$ and -1 are equal, the minimum error probability detector can be expressed as:

$$\text{decide } \mathcal{H}_1 \text{ if } \hat{b} = \text{Re}(\mathbf{d}^\dagger \mathbf{V}_r^\dagger \mathbf{V}_r \mathbf{Z}) > 0. \tag{11}$$

5. PERFORMANCE ANALYSIS

Defining $\mathbf{\Sigma} = \frac{1}{\sigma_W^2} \sqrt{\mathbf{\Delta}_r} \mathbf{V}_r E[(\mathbf{d} - E[\mathbf{d}])(\mathbf{d} - E[\mathbf{d}])^\dagger] \mathbf{V}_r^\dagger \sqrt{\mathbf{\Delta}_r}^\dagger$, if $\mathbf{\Sigma}$ is full rank, using the minimum error probability detector rule in (11), the average bit error rate (BER) can be given by [8]:

$$P_b = \frac{1}{\pi} \int_0^{\frac{\pi}{2}} \left[\det \left(\frac{\mathbf{\Sigma}}{\sin^2\theta} + \mathbf{I} \right) \right]^{-1} e^{-\mathbf{m}^\dagger (\mathbf{\Sigma} + \sin^2\theta \, \mathbf{I})^{-1} \mathbf{m}} d\theta \, . \tag{12}$$

where $\mathbf{m} = \frac{1}{\sigma_W} \sqrt{\mathbf{\Delta}_r} \mathbf{V}_r E[\mathbf{d}]$. The potential diversity order is given by N_r, which is the rank of $\mathbf{P}$. Because the modes are more difficult to discriminate in higher frequency bands, the rank of $\mathbf{P}$ decreases as the transmission frequency band increases.

The BER simulation is shown in Fig. 4, using $d = 50$ m, $u = 1500$ m/s and $r = 15$ km. The simulation results show the BER and diversity performances of three transmission frequency bands: 1–2 kHz, 5–6 kHz and 7–8 kHz. As we can see, the BER performance deteriorates and the diversity order decreases when the transmission frequency band increases. For comparison, we also show the receiver performance when the matched filter is not matched to the characteristic function of the environment. Assuming that we do not have any information about the dispersive modes, we use the impulse as the matched filter. As we can see, large performance deterioration can be observed in the BER curve marked by diamonds in Fig. 4. The reason for this is that, when the receiver's waveform does not match the transmitted waveform, the waveform correlation matrix $\mathbf{P}$ is not a Hermitian matrix. Thus, the detection rule needs to be modified to accommodate the change in the waveform.

6. CONCLUSION

We developed a frequency domain characterization of shallow water environments and analyzed its dispersive characteristics. Following this model, we developed the corresponding waveform and receiver to exploit the diversity existing in the system characterization. Simulation results demonstrated that the diversity and BER performances were improved by the aforementioned waveform and receiver design schemes.

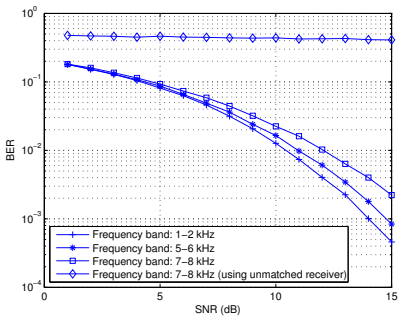

Fig. 4. BER performance in different transmission bands and comparison to the performance of an unmatched receiver.

7. REFERENCES

[1] C. Chen, J. H. Miller, G. F. Bourdreaux-Bartels, G. R. Potty, and C. J. Lazauski, "Time-frequency representations for wideband acoustic signals in shallow water," in *Oceans*, Sept. 2003, vol. 5, pp. 2903–2907.

[2] Y. Jiang and A. Papandreou-Suppappola, "Discrete time-frequency models of generalized dispersive systems," in *IEEE Int. Conf. on Acoustic, Speech and Signal Processing*, May 2006, vol. 3, pp. 349–352.

[3] L. R. LeBlanc and P.-P. J. Beaujean, "Spatio-temporal processing of coherent acoustic communication data in shallow water," *IEEE Journal of Oceanic Engineering*, vol. 25, pp. 40–51, Jan. 2000.

[4] G. F. Edelmann, H. C. Song, S. Kim, W. S. Hodgkiss, W. A. Kuperman, and T. Akal, "Underwater acoustic communications using time reversal," *IEEE Journal of Oceanic Engineering*, vol. 30, pp. 852–864, Oct. 2005.

[5] L. J. Ziomek, *Fundamentals of Acoustic Field Theory and Space-Time Signal Processing*, CRC Press, 1999.

[6] A. L. Maggi and A. J. Duncan, "Underwater acoustic propagation modelling software - actup v2.2l," http://www.cmst.curtin.edu.au/products/actoolbox/.

[7] R.G. Baraniuk and D.L. Jones, "Unitary equivalence: a new twist on signal processing," *IEEE Transactions on Signal Processing*, vol. 43, no. 10, pp. 2269–2282, Oct. 1995.

[8] V. V. Veeravalli, "On performance analysis for signaling on correlated fading channels," *IEEE Transactions on Communications*, vol. 49, pp. 1879–1883, Nov. 2001.